

Strength analysis of carbon fiber reinforced polymer and titanium alloy for axisymmetric lap joint

Many industries such as oil, gas, aerospace, and automotive, use axisymmetric adhesively bonded single lap joints. Different materials are frequently mated using axisymmetric lap joints. When composite adherents delaminate, the stress circulation inside the adhesive layer significantly influenced. As a result, the importance of considering adhesive layer stresses in the presence of considerable delamination is investigated in this paper. To understand stress analysis and examine adhesive bond strength at static loading conditions, the model created using finite element analysis with cohesive zone modelling. A complete parametric study carried using simple finite element code in ABAQUS, the axisymmetric single lap joints adhesively bonded joints prepared with different material adherents. Analysis carried on the influence of numerous factors such as the distribution stress inside the adhesive joints. In this connection, mating of carbon reinforced polymer composite to titanium alloy adherends discussed thoroughly. The results show that depending on the position of the delamination, the presence of a throughout-the-thickness delamination affects the structural response of both single lap and axisymmetric adhesively bonded joints by varying overlap length. The presence of a delamination reduced adhesive peel and shear stresses significantly in both joint configurations.

Keywords: Axisymmetric lap joint, carbon fiber, titanium alloy, finite element analysis.

1.0 Introduction

Composite materials are widely used in the aerospace and aviation industries due to their light weight and great strength. Carbon reinforced polymer composite (CFRPC) is a composite material which has high strength and low weight good aesthetic characteristics. The Boeing 787 Dreamliner and Airbus350XB contains 50% to 53% composite

material in structures, due to this the fuel consumption will be decreases up to 20% [1, 2]. Adhesive bonding has several advantages, including more constant stress distribution and the ability to fabricate joints from a variety of materials that would be difficult to do with other methods [3]. Adhesive bonding is considerably light weight as compared to bolts, rivets, and other common mechanical joints. Cost savings, superior corrosion and fatigue resistance, fracture delay, reasonable damping qualities, and the benefit of varied adherents thermal expansions are all advantages of this joint. Prior to adhesive failure, a peel stress occurs at adhesively bonded joints, causing failure inside the composite in transverse with the composite in transverse tension. As a result of these peel stresses cracking the composite adherends apart locally, the shear transmission capability between the inner and outer adherents is eliminated [4]. Venkatesha B K et al. [5] studied the modelling and simulation of crack initiation, crack growth, and crack arrest features in the stiffened panel. Finite element analysis (FEA) is a computational method this will maintain complicated configurations and non-linear material properties, reducing the need for costly investigational procedures [6]. The cohesive zone models (CZMs) which is used as a numerical approach, because in which very easy to simulation of crack initiation, crack propagation and failure of the material. The crack initiation and failure of the material follows energetic criteria, in which behaviour of the material modelled by using cohesive law with dissimilar shape material [7]. This method is based on the failure-direction traction-separation rule, which states that as interface separation grows, traction along the interface reaches a maximum and then gradually decreases, allowing the fracture to propagate and the bond to debone [8]. According to previous studies, joint strength increases as the bond-line thickness decreases until it reaches a particular bond-line thickness. This is in addition to the increased bending moment that thick bond-line completes because of the increased loading offset [9]. This is related to the increased bending moment of the thick bond-line due to the increased loading offset. Only bond parameters were explored by Neto et al.[4] and Ribeiro et al.[7], who took into account the bulk adhesive's cohesive failure in single-lap joints (SLJ). Interfacial damage between the adherents and the

Messrs. Nagayya, PG Scholar, Department of Mechanical Engineering, DSCE, M.K Venkatesh and Nithesh Bhaskar N, Assistant Professor, Department of Mechanical Engineering, DSCE and Venkatesha B K, Assistant Professor, School of Mechanical Engineering, REVA University, Bengaluru, India. E-mail: anagayyav9747@gmail.com / bmkvenkateshme@dayanandasagar.edu / cnithesh-me@dayanandasagar.edu / dvenkatesharvc@gmail.com;https://orcid.org/0000-0003-2315-0880

adhesive was not considered. Pires et al. [10] and Breto et al. [11] investigated functionally graded adhesive (FGA) and hybrid adhesive, and found that utilising FGA and hybrid adhesive, the stress concentration at the overlap region could be reduced. However, they have not been tested to see if they may predict progressive interfacial breakdown numerically. Carbas et al. [12] also studied FGA joint by means of induction heating. From the results they conclude that grading can be achieved by induction heating by this the strength of the joint should be increased. In previous literature, study of interfacial failure for tubular-lap joint (TLJ) not considered. Against this, undertaken the study of tubular-lap joint using carbon fiber reinforced polymer and titanium alloy.

TABLE 1: MECHANICAL PROPERTIES OF THE 7779 ADHESIVE [14]

Mechanical properties	Value
E(MPa)	1169
G(MPa)	389
GT(N/mm)	2.75
GS(N/mm)	2.03

TABLE 2: MECHANICAL PROPERTIES OF THE CFRP ADHEREND [14]

Mechanical properties	Value
E1 (MPa)	26580
E2 (MPa)	26580
E3 (MPa)	3880
ν_{12}	0.35
ν_{13}	0.3
ν_{23}	0.3
G12 (MPa)	8482
G13 (MPa)	3678
G23 (MPa)	3678

2.0 Numerical approach

2.1 AXISYMMETRIC LAP JOINT (ALJ) MODEL

ALJ is created in CATIA utilising part modelling and then exported to ABAQUS for FEA analysis. The CFRP adherent was modelled using mechanical properties shown in Table 2, the adhesive used was Ashland's 7779, which is a two-component polyurethane structural adhesive. The mechanical properties of 7779 adhesive are shown in Table 1.

The adhesive and adherents were developed with 4-node axisymmetric components (CAX4). For interlaminar contacts and adhesive, four-node axisymmetric cohesive elements (COHAX4) are used. Surface-base tie constrains are used to join the cohesive parts. It is advantageous because modelling the adhesive material as an elastic-plastic material is a correct and good approach. For example, Mahoney et al. [13] applied the elastic-plastic material for the adhesive and only studied the interfacial damage and considered the adhesive as a linear-elastic material. But they are not considering the failure of adhesive material. The modelling

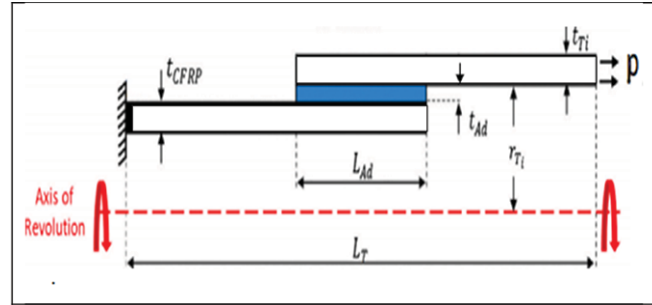


Fig.1: Axisymmetric modelling for SLJ loading and boundary conditions

will be done such that it should be similar to SLJ. The structure, however, would behave like an ALJ when matched with Abaqus axisymmetric modelling. It was possible to resolve the adherends after part modelling building them with their length (L_T) corresponding to the axis of revolution, the radius of the axisymmetric adhesive bond lap structure is dependent on the length from the axis of revolution, resulting in an axisymmetric adhesive bond lap structure. Resulting in an axisymmetric adhesive bond lap structure with the radius of the axisymmetric being dependent on the length from the axis of revolution. The ALJ was confined in the following way: one end was fixed, while the other was subjected to the load described in Fig.1.

The following values used to create geometric modelling,

- $r_{TI} = 19\text{mm}$.
- $L_T = 153\text{mm}$.
- $LAD = 53\text{mm}, 63\text{mm}$
- $t_{CFRP} = 1\text{mm}$.
- $t_{TI} = 0.9\text{mm}$.
- $t_{AD} = 0.50, 0.75, 1\text{mm}$.

3.0 Results and discussions

3.1. OVERLAP LENGTH

Varying the overlap length while keeping the adhesive thickness constant determines the adhesive bond strength.

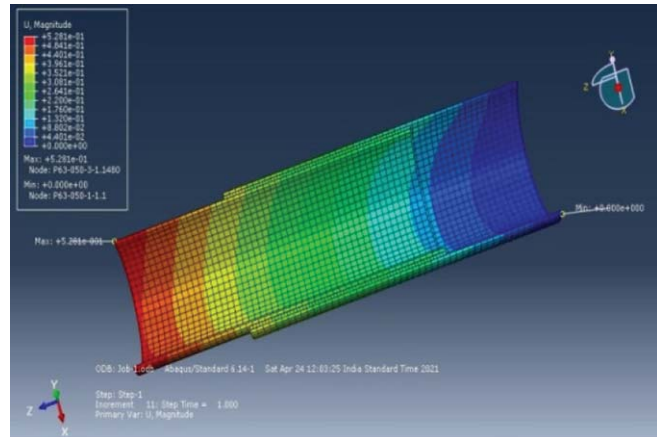


Fig.2: Axisymmetric single lap joint of adhesive bond deformation in trial 1

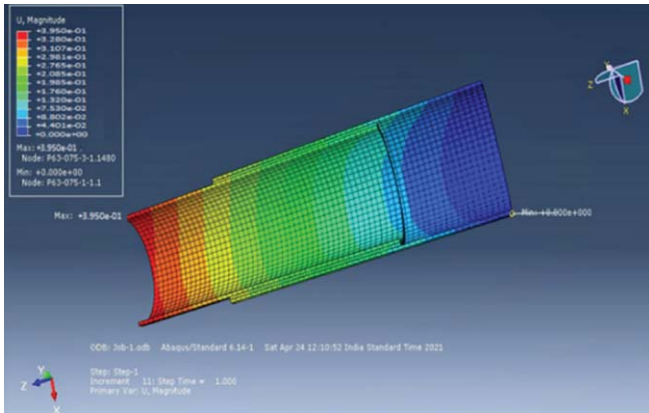


Fig.3: Axisymmetric single lap joint of adhesive bond deformation in trial-4

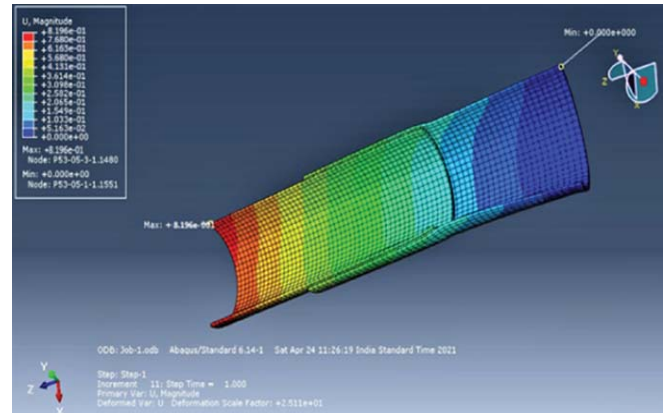


Fig.6: Axisymmetric single lap joint of adhesive bond deformation in trial-3

The maximum deformation for 0.5mm thickness of adhesive is obtained that 0.582mm and 0.395mm is shown in Figs.2, and 3, respectively with varying the overlap length. The deformation goes decreases when overlap length increases.

3.2. OVERLAP THICKNESS

The thickness of the adhesion line, which represents the union line, contributes greatly to the plate's resistance to shear stress. The displacements in proportion to adhesive thickness increase as the overall strength of the joint increases, which implies that the displacement in relation to adhesive thickness is bigger in thin joints and reduces

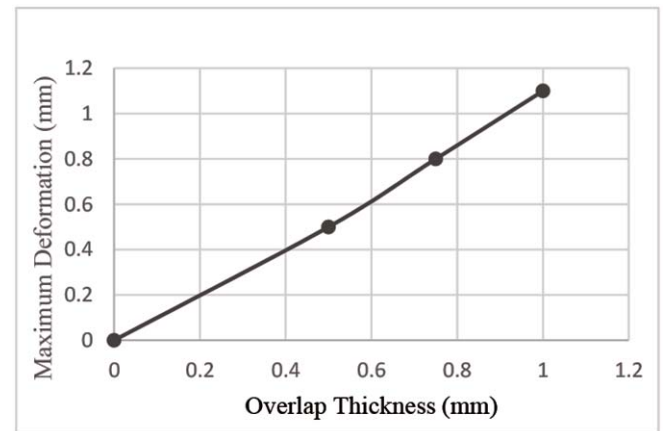


Fig.7: Adhesive bond deformation varying with thickness of the bond at overlap length of 53mm

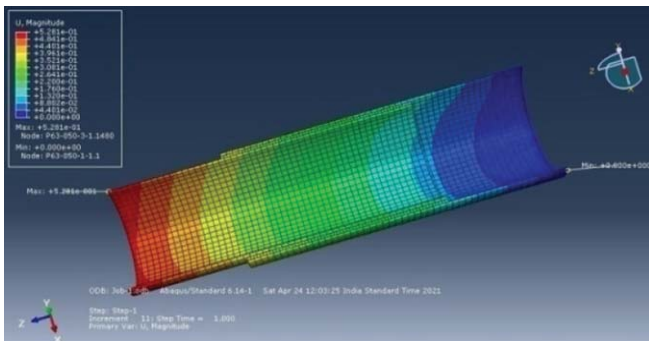


Fig.4: Axisymmetric single lap joint of adhesive bond deformation in trial-1

progressively as the total strength of the joint increases. Adhesive bond deformation varying with thickness of the bond at Overlap length is 53mm is shown in Fig.7. Axisymmetric Single lap adhesive joint of overlap length 53mm and thickness of adhesive is 0.50, 0.75, 1mm at that case deformation as shown in Figs.4, 5, and 6, respectively.

Similarly axisymmetric single lap adhesive joint of overlap length 63mm and thickness of adhesive is 0.50mm, 0.75mm, 1mm at that case deformation obtained is shown in Figs.8, 9

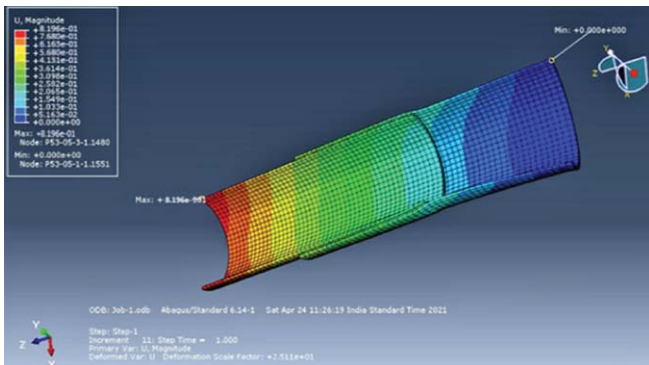


Fig.5: Axisymmetric single lap joint of adhesive bond deformation in trial-2

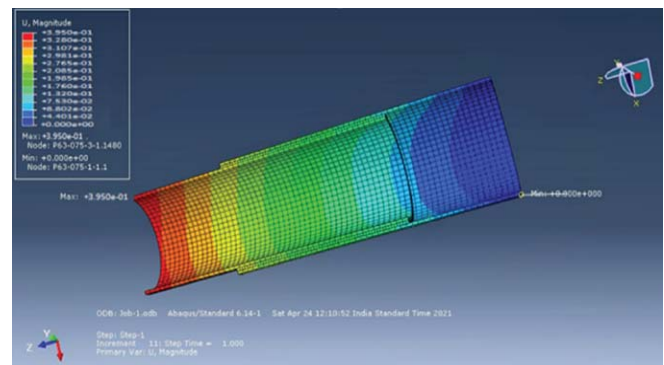


Fig.8: Axisymmetric single lap joint of adhesive bond deformation in trial-4

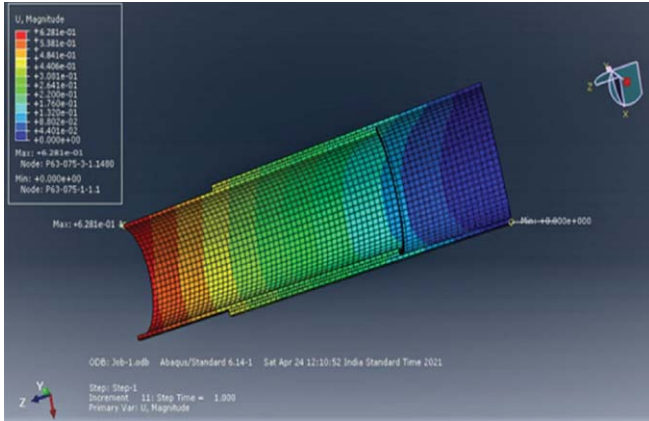


Fig.9: Axisymmetric single lap joint of adhesive bond deformation in trial-5

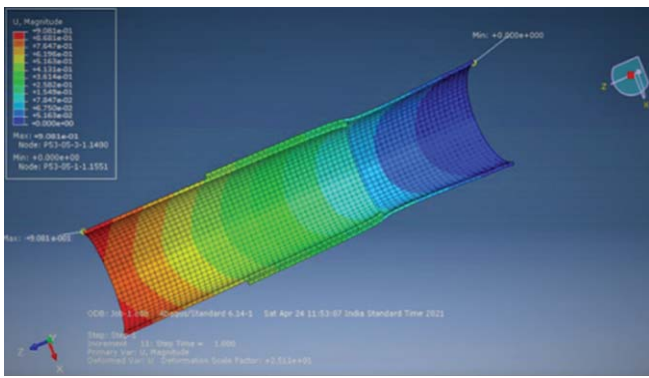


Fig.10: Axisymmetric single lap joint of adhesive bond deformation in trial-6

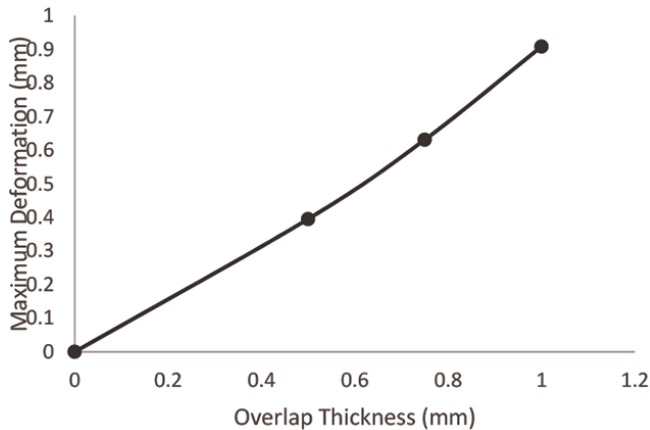


Fig.11: Deformation of adhesive bonds at an overlap length of 63mm, the bond thickness varies

and 10 at constant load applied and that variation is shown in Fig.11. The effect that occurs in the direction of the length of adhesive bond is assessed, and only a decrease in extreme stress is obtained, according to the data acquired through the method of adhesive bonding. Finally, when the adhesive bonding thickness is changed, the behaviour demonstrates that effective stresses are reduced along the lap length. The obtained stress in all cases presented in Table 3.

TABLE 3: STRESS OBTAINED FOR DIFFERENT THICKNESS OF ADHESIVE BONDING AND OVERLAP LENGTH AT STATIC LOADING CONDITION

Thickness of adhesive bond (mm)	Stress (MPa) obtained for overlap length of	
	53mm	63mm
0.50	18.83	20.2
0.75	17.6	17.5
1	16.7	15.2

4.0 Conclusions

From the numerical simulation study of axisymmetric single lap joint of adhesive bond using ABAQUS finite element software, the following conclusions are made.

- Maximum stress and maximum deformation decrease when increasing the thickness of the adhesive at constant overlap length.
- If overlap length and thickness of the adhesive bond increased and stress decreased and strength also high at that case as compared to others.
- If overlap length of the adhesive bond changed and thickness of adhesive bond constant the maximum deformation decreases.

References

- [1] Boeing 787 Dreamliner (2021): <https://www.boeing.com/commercial/787/bydesign/#/advanced-composite-use>.
- [2] Airbus A350XW Family (2021): <https://www.airbus.com/aircraft/passenger-aircraft/a-350xb-family.html>.
- [3] Valente JPA Campilho R.D.S.G., Marques E.A.S., Machado J.J.M. and Silva L.F.M. (2019): Adhesive Joint Analysis under Tensile impact Loads by Cohesive Zone Modeling. *Journal of Composite Structures*, 222,110894.
- [4] Neto J.A.B.P., Campilho R.D.S.G. and da Silva L.F.M. (2012) Parametric Study of Adhesive Joints with Composites. *International Journal of Adhesion and Adhesives*, 37, 96–101.
- [5] Venkatesha B K, Prashanth K P and Deepak Kumar T. (2014): Investigation of Fatigue Crack Growth Rate in Fuselage of Large Transport Aircraft using FEA Approach, *Global Journal of Research in Engineering-USA*, ISSN: 2249-4596, 14(1), 11-19.
- [6] He X. (2011): A Review of Finite Element Analysis of Adhesively Bonded Joints. *International Journal of Adhesion and Adhesives*. 31(4), 248–264.
- [7] Ribeiro TEA, Campilho RDG, da Silva LFM, & Goglio L. (2016). Damage Analysis of Composite-Aluminum Adhesively-bonded Single-Lap Joint. *Journal of Composite Structures* 136, 25–33.

- [8] Da Silva L.F.M, Campilho R..D.SG. and Vassilopoulos A.P. (2015) Fatigue and Fracture of Adhesively-Bonded Composite Joints. Woodhead Publishing. 43-71.
- [9] Grant LDR, Adams RD and Da Silva L.F.M. (2009): Experimental and Numerical Analysis of Single Lap Joints for the Automotive Industry. *International Journal of Adhesion and Adhesives* 29, 405–413.
- [10] Pires I., Quintino L., Durodola J.F. and Beevers A. (2003): Performance of Bi-adhesive Bonded Aluminum Lap Joints. *International Journal of Adhesion and Adhesives* 23, 215–223.
- [11] Breto R., Chiminelli A., Duvivier E., Lizaranzu M. and Jimenez M.A. (2015): Finite Element Analysis of Functionally Graded Bond-lines for Metal/Composite Joints. *International Journal of Adhesion and Adhesives* 91, 920–936.
- [12] Carbas R.J.C. and da Silva L.F.M, Critchlow G.W. (2014): Adhesively Bonded Functionally Graded Joints by Induction Heating”. *International Journal of Adhesion and Adhesives* 48,110–118.
- [13] O’Mahoney D.C., Katnam K.B., O’Dowd N.P., McCarthy C.T. and Young T.M. Taguchi (2013): Analysis of Bond Composite Single-Lap Joint using a Combined Interface-Adhesive Damage Model. *International Journal of Adhesion and Adhesives* 40, 168–178
- [14] Kai Wai, Yiwei chen, Maojun Li and Xujing Yang.(2018) Strength and Failure Mechanism of Composite-Steel Adhesive Bond Single Lap joints. *Advances in Material Science and Engineering*.
-